THE ASTROPHYSICAL JOURNAL, 474:639–649, 1997 January 10

THE HIGH-ENERGY CONTINUUM EMISSION OF THE GAMMA-RAY BLAZAR PKS 0528+134

RITA M. SAMBRUNA[1]
NASA/GSFC, Code 662, Greenbelt, MD 20771

C. MEGAN URRY
Space Telescope Science Institute, 3700 San Martin Drive, Baltimore, MD 21218

L. MARASCHI
Osservatorio Astronomico di Brera, via Brera 28, I-20128, Milano, Italy

G. GHISELLINI
Osservatorio Astronomico di Brera, via Brera 28, Milano, Italy

R. MUKHERJEE[2]
NASA/GSFC, Code 661, Greenbelt, MD 20771

JOSEPH E. PESCE
Space Telescope Science Institute, 3700 San Martin Drive, Baltimore, MD 21218

S. J. WAGNER[3]
Landessternwarte Königstuhl, 69117 Heidelberg, Germany

A. E. WEHRLE
Infrared Processing and Analysis Center, California Institute of Technology, 100-22, Pasadena, CA 91125

R. C. HARTMAN
NASA/GSFC, Code 661, Greenbelt, MD 20771

Y. C. LIN
High-Energy Physics Laboratory, Stanford University, Stanford, CA 94305

AND

C. VON MONTIGNY[1]
NASA/GSFC, Code 662, Greenbelt, MD 20771
Received 1996 May 14; accepted 1996 July 31

ABSTRACT

We present *Advanced Satellite for Cosmology and Astrophysics* (*ASCA*) observations of the γ-ray blazar PKS 0528+134, obtained at two separate epochs in 1994 August and 1995 March. These data represent the first measurement of the X-ray continuum emission of this source in the medium-hard X-ray band. Both *ASCA* spectra are consistent with a single power law with photon index $\Gamma \sim 1.7$–1.8 and column density $N_{\rm H} \sim 5 \times 10^{21}$ cm^{-2}, higher than Galactic. The X-ray flux increased by a factor of 4 in ~ 7 months without appreciable change of the spectral shape. During the lower state of 1994 August, PKS 0528+134 was observed simultaneously in the optical, X-rays, and at γ-ray energies with EGRET. The γ-ray intensity is the faintest detected thus far in the source, with a steep spectrum ($\Gamma \sim 2.7$). The extrapolation of the X-ray continuum to the γ-ray range requires a sharp spectral break at $\sim 10^{22}$ Hz.

We discuss the radio through γ-ray spectral energy distribution of PKS 0528+134, comparing the low state of 1994 August with the flare state of 1993 March. We show that in PKS 0528+134, a non-negligible contribution from the external radiation field is present and that, although synchrotron self-Compton scenarios cannot be ruled out, inverse Compton upscattering of thermal seed photons may be the dominant cooling process for the production of the high-energy continuum in this blazar.

Subject headings: galaxies: active — galaxies: individual (PKS 0528+134) — gamma rays: observations — radiation mechanisms: nonthermal — X-rays: galaxies

1. INTRODUCTION

PKS 0528+134 is a compact radio-loud quasar at a redshift $z = 2.07$ (Hunter et al. 1993). Its emission in the radio and optical bands is weakly polarized, $\sim 1\%$–2% and $\lesssim 0.3\%$, respectively (Perley 1982; Fugmann & Meisenheimer 1988). The source classification changed abruptly in early 1991 from gigahertz-peaked spectrum (GPS) to blazar with a core-jet structure (Zhang et al. 1994; Pohl et al. 1996). Superluminal motion, with $\beta_{\rm app} \sim 4$, has been recently measured in PKS 0528+134 (Pohl et al. 1996).

Historical light curves in the radio and millimeter bands show that the emission of PKS 0528+134 at these frequencies varies on timescales of years (Aller et al. 1985; Steppe et al. 1993; Marscher et al. 1994). In the optical, the source is faint, having a thus far observed magnitude $V = 19.5$ mag (Wall & Peacock 1985). Optical observations are made difficult by the high Galactic extinction, $A_V = 2.3$,

[1] NAS/NRC Research Associate.
[2] Universities Space Research Association.
[3] Visiting Astronomer, Calar Alto Observatory, Deutsche–Spanische Astronomiches Zentrum.

in the direction of PKS 0528+134 because this source is located at a low Galactic latitude and behind a translucent molecular cloud (Liszt & Wilson 1993). Extinctions as high as $A_V = 5$ are suggested by X-ray observations with *ROSAT* (Zhang et al. 1994). An optical absorption system of low-ionization lines is present along the line of sight at $z = 1.57$ (Hunter et al. 1993).

PKS 0528+134 is one of the brightest active galactic nuclei (AGNs) and the second most distant quasar detected with the EGRET experiment on board the *Compton Gamma Ray Observatory* (*CGRO*) (Hunter et al. 1993; Thompson et al. 1995). The emission in the 30 MeV–30 GeV energy band is variable, with flux changes of a factor of 3 in ~ 2 yr and smaller amplitude variations on a timescale of a few days (Mukherjee et al. 1996 and references therein). Flux changes in γ-rays are accompanied by γ-ray spectral variability in the sense of the EGRET spectrum becoming harder as the source brightens (Mukherjee et al. 1996). PKS 0528+134 was also detected with OSSE in the 0.05–1.0 MeV band (McNaron-Brown et al. 1995) and with COMPTEL above 10 MeV (Collmar et al. 1993), while at TeV energies only an upper limit to the flux was obtained (Kerrick et al. 1995). The power emitted at MeV–GeV frequencies often exceeds the power at lower energies (von Montigny et al. 1995; Mukherjee et al. 1996), making the study of the high-energy continuum of PKS 0528+134 of great interest. The huge high-energy output together with its fast variability require that the emission from PKS 0528+134 is relativistically beamed, with a Doppler factor in the γ-ray region $\delta \gtrsim 5.8$ (Dondi & Ghisellini 1994; see also Zhang et al. 1994).

We observed PKS 0528+134 for the first time in a medium-hard X-ray range (0.4–10 keV) with the *Advanced Satellite for Cosmology and Astrophysics* (*ASCA*) on two separate occasions, in 1994 August and 1995 March, during coordinated γ-ray pointings with *CGRO* EGRET. Optical observations, overlapping with the 1994 August *ASCA* and EGRET pointings, were also taken. In this paper, we present both *ASCA* observations of PKS 0528+134, together with the optical and EGRET data of 1994 August.

The analysis of the *ASCA* data of PKS 0528+134 is described in § 2, while in § 3 the optical and EGRET observations simultaneous to the *ASCA* pointing of 1994 August are presented. In § 4, we construct the spectral energy distribution of PKS 0528+134. The results of this work are summarized and discussed in §§ 5 and 6, respectively. Our conclusions are given in § 7. Throughout this paper, $H_0 = 75$ km s^{-1} Mpc^{-1} and $q_0 = 0.5$ are assumed.

2. *ASCA* OBSERVATIONS

2.1. *Data Reduction and Analysis*

We observed PKS 0528+134 with *ASCA* on 1994 August 28 and on 1995 March 19. For a description of the *ASCA* payload, see Tanaka, Inoue, & Holt (1994). The solid-state imaging spectrometers (SIS0 and SIS1) operated in mixed faint and bright mode for 20 ks in 1994 August and for 22.4 ks in 1995 March, while the gas-imaging spectrometers (GIS2 and GIS3) were used in pulse-height mode for 21.4 ks and 24.4 ks at the two epochs, respectively. The 1994 August observation was performed with the SIS in 2 CCD mode (i.e., two chips were used), while the 1995 March data were taken with the SIS in 1 CCD mode. In order to increase the statistics, we combined the SIS bright data with the SIS faint data after the latter were converted into "BRIGHT." No echo or dark frame error corrections were applied (see The ABC Guide to *ASCA* Data Reduction, v.4, 1995 March).

The data were reduced by applying a number of standard screening criteria. For the 1994 August data set, we rejected the data accumulated during passage of the South Atlantic Anomaly in intervals of Earth, angular distance, and elevation angles lower than 20′, 0.°01, and 10′, respectively, as well as when the geomagnetic rigidity was lower than 6 GeV/c (for a description of these parameters see The ABC Guide to *ASCA* Data Reduction, v.4, 1995 March). In the case of the 1995 March data, the angular distance (which measures the wobbling of the satellite around the pointing direction) was higher than nominal, up to 0.°02, in the first 10,000 s of the exposure. In order to include these data in the analysis, a threshold of 0.°02 was used. The 1995 observation also had two telemetry losses, in the middle and at the end of the exposure, and 2000 s of data in total were lost. Only grades 2, 3, and 4 were retained for the analysis in both data sets. The effective exposures and corresponding source count rates after screening are reported in Table 1. During the 1995 March observation, the source was a factor of ~ 4 brighter than 7 months earlier in 1994 August.

The source spectra were extracted from circular regions centered on the source position with radius 4′ for the SIS and 6′ for the GIS, which has a larger intrinsic point-spread function. In the case of the GIS, we evaluated the background in circular regions of radius 4′ located about 12′ away from the target, where the source count contamination is negligible. In the case of the SIS, the background was evaluated in a circular region of radius 2′ located 6′ away from the target on the same chip. The background count rates are 2% (SIS) and 10% (GIS) of the source intensity during the higher state of 1995 March, and 11% (SIS) and 14% (GIS) during the low state of 1994 August.

The SIS and GIS spectra were rebinned with a minimum of 20 counts in each spectral bin to validate the use of the χ^2 statistic. In order to increase the signal-to-noise ratio, we performed joint fits to the data from the four detectors, leaving only the normalizations as independent parameters. The 1994 November and 1994 May response matrices were used for the SIS and GIS spectra, respectively. The first 14 channels of the SIS and 69 channels of the GIS (energies up to 0.4 and 0.7 keV, respectively) were excluded from the analysis since the spectral calibrations of the detectors are poorly known in these energy ranges. In the case of the SIS, further excluding the data below 0.6 keV, where a residual

TABLE 1

LOG OF *ASCA* OBSERVATIONS

Detector	Exposure (s)	Count Rate (counts s^{-1})
1994 August 28, 14:20 UT		
SIS0	19,511	0.072 ± 0.002
SIS1	18,406	0.054 ± 0.002
GIS2.....	21,030	0.053 ± 0.002
GIS3.....	20,987	0.060 ± 0.002
1995 March 19, 14:22 UT		
SIS0	17,521	0.314 ± 0.007
SIS1	17,579	0.253 ± 0.005
GIS2.....	18,064	0.207 ± 0.004
GIS3.....	18,062	0.248 ± 0.005

calibration problem seems to be present, yields fitted absorption column densities only 2% different than when these data are included in the analysis. The SIS data below 0.6 keV were therefore retained in the spectral analysis.

2.2. *Timing Analysis*

No flux variability was detected within each single *ASCA* exposure. The χ^2 test yields probabilities of $\gtrsim 11\%$ and $\gtrsim 40\%$ that the light curve is constant of for the two SIS and for GIS2 at both epochs, respectively. A smaller probability is obtained for GIS3: $\sim 6\%$ in 1995 March and $\sim 0.3\%$ in 1994 August. A visual inspection of the two GIS3 light curves shows that this is the result of local flux fluctuations occurring ~ 5000 s after the observation started at both epochs; no corresponding changes are present in the simultaneous GIS2 and SIS light curves. Therefore, we regard as unlikely the possibility that these fluctuations are intrinsic to the source, and we attribute them to instrumental effects.

From linear fits to the *ASCA* light curves, we can exclude at 99% confidence the presence of flux changes with amplitude $\gtrsim 33\%$ for the SIS and $\gtrsim 48\%$ for the GIS on timescales $\lesssim 5$ and $\lesssim 1.6$ hr for 1994 August and 1995 March, respectively.

2.3. *Spectral Fits to the ASCA Data*

The *ASCA* data were fitted with a single power law absorbed at the low energies by a column density of cold gas $N_{\rm H}$. In the spectral fits, $N_{\rm H}$ was left both free and fixed to the total Galactic (atomic + molecular) H I column density along the line of sight, 3.9×10^{21} cm^{-2} (see below). We used the Morrison & McCammon (1983) cross section for photoelectric absorption, where abundances of neutral elements other than hydrogen are fixed at solar values. The results of the spectral fits are reported in Table 2 together with the 90% confidence errors for one parameter of interest ($\Delta\chi^2 = 2.7$). All quoted quantities are in the observer's frame.

Assuming an entirely local (i.e., $z = 0$) absorber, at both epochs the fits with free $N_{\rm H}$ are preferred with high confidence from the F-test ($\gtrsim 98\%$ in 1994 August; $>99\%$ for 1995 March) with respect to the fits with fixed Galactic column density. The data with the folded model for the free $N_{\rm H}$ fits are shown in Figures 1*a* and 1*b* for the two data sets, while the corresponding residuals are shown in Figures 1*c* and 1*d*. The fitted $N_{\rm H} \sim 5 \times 10^{21}$ cm^{-2} is in excess of the Galactic value at $\sim 95\%$ confidence for the 1994 August and $>99\%$ for the 1995 March observations (Fig. 2), confirming earlier reports for excess absorption based on *ROSAT* observations (Zhang et al. 1994; Mukherjee et al. 1996). The fitted *ASCA* photon index ($\Gamma \sim 1.7$–1.8) is in good agreement with the average slopes of highly polarized/optically violently variable quasars at medium-hard energies measured with *Ginga* and *EXOSAT* (Ohashi et al. 1989; Sambruna et al. 1994). Within the uncertainties, the continuum photon index does not change between the 1994 August observation and the 1995 March observation, when the source was brighter by a factor of 4; $\Delta\Gamma \lesssim 0.2$ at 90% confidence for a fixed column density in the range of overlap of the confidence contours (Fig. 2).

The flux densities at 1 keV and integrated 2–10 keV fluxes in SIS0 are reported in Table 2. Assuming isotropic rest-frame emission, the observed 2–10 keV fluxes from *ASCA* imply apparent source luminosities of 9.5×10^{46} and 3.2×10^{47} ergs s^{-1} for the 1994 August and 1995 March observations, respectively.

We next fitted the *ASCA* data with a single power law and an absorber at a redshift z, which was allowed to vary between 0 and 2.07 (the redshift of PKS 0528+134). A second absorber at $z = 0$, fixed at 3.9×10^{21} cm^{-2}, was added to take into account the Galactic contribution. In both data sets, because of the limited statistics of the data below 1 keV, it was not possible to constrain the location of the absorber. That is to say, there is no statistical preference among local ($z = 0$), rest frame ($z = 2.07$), or intervening absorbers. Higher signal-to-noise ratios at low energies are required to distinguish among these possibilities (e.g., Serlemitsos et al. 1994).

We investigated models that can fit the *ASCA* data with Galactic absorption only. A broken power law with fixed Galactic absorption gives a fit statistically equivalent to the single power law + free $N_{\rm H}$ (Table 2) because both models give a convex (downward curved) spectrum. For the broken power law, the low-energy slope is very flat and it is consistent with a rising energy spectrum.

Any iron emission lines from PKS 0528+134, emitted in the rest frame between 6.4 keV (Fe I) and 6.7 keV (Fe XXV), would be observed in the 2.08–2.18 keV energy range where the SIS sensitivity is best. No emission lines are detected in this range in either *ASCA* data sets of PKS 0528+134, with formal 90% upper limits on the rest-frame equivalent width of $\lesssim 172$ eV (Fe I) and $\lesssim 50$ eV (Fe XXV) in both data sets. This confirms previous findings based on *Ginga* data that

TABLE 2

FITS TO THE *ASCA* SPECTRA OF PKS 0528+134

Model	$N_{\rm H}$ (10^{21} cm^{-2})	Γ_1	Γ_2	E_0 (keV)	χ^2_r/dof	$F_{1\,\rm keV}$ (μJy)	$F_{2-10\,\rm keV}$ (10^{-11} ergs cm^{-2} s^{-1})
			1994 August				
Power law.....	3.9 (fix)[a]	1.53 ± 0.05	...	...	1.08/232		
	$5.06^{+0.93}_{-0.70}$	$1.65^{+0.12}_{-0.08}$	...	...	1.05/231	0.57 ± 0.08	$0.35^{+0.08}_{-0.04}$
Broken power law.....	3.9 (fix)[a]	$1.16^{+0.25}_{-2.28}$	$1.63^{+0.12}_{-0.08}$	1.73 ± 0.45	1.05/230		
			1995 March				
Power law.....	3.9 (fix)[a]	1.60 ± 0.03	...	...	0.97/625		
	$5.57^{+0.41}_{-0.39}$	1.79 ± 0.05	...	...	0.88/624	2.26 ± 0.16	$1.2^{+0.1}_{-0.2}$
Broken power law.....	3.9 (fix)[a]	$0.95^{+0.25}_{-0.24}$	$1.48^{+0.27}_{-0.11}$	$1.70^{+0.05}_{-0.03}$	0.88/623		

[a] Total atomic and molecular column density in the direction of PKS 0528+134 (see text).

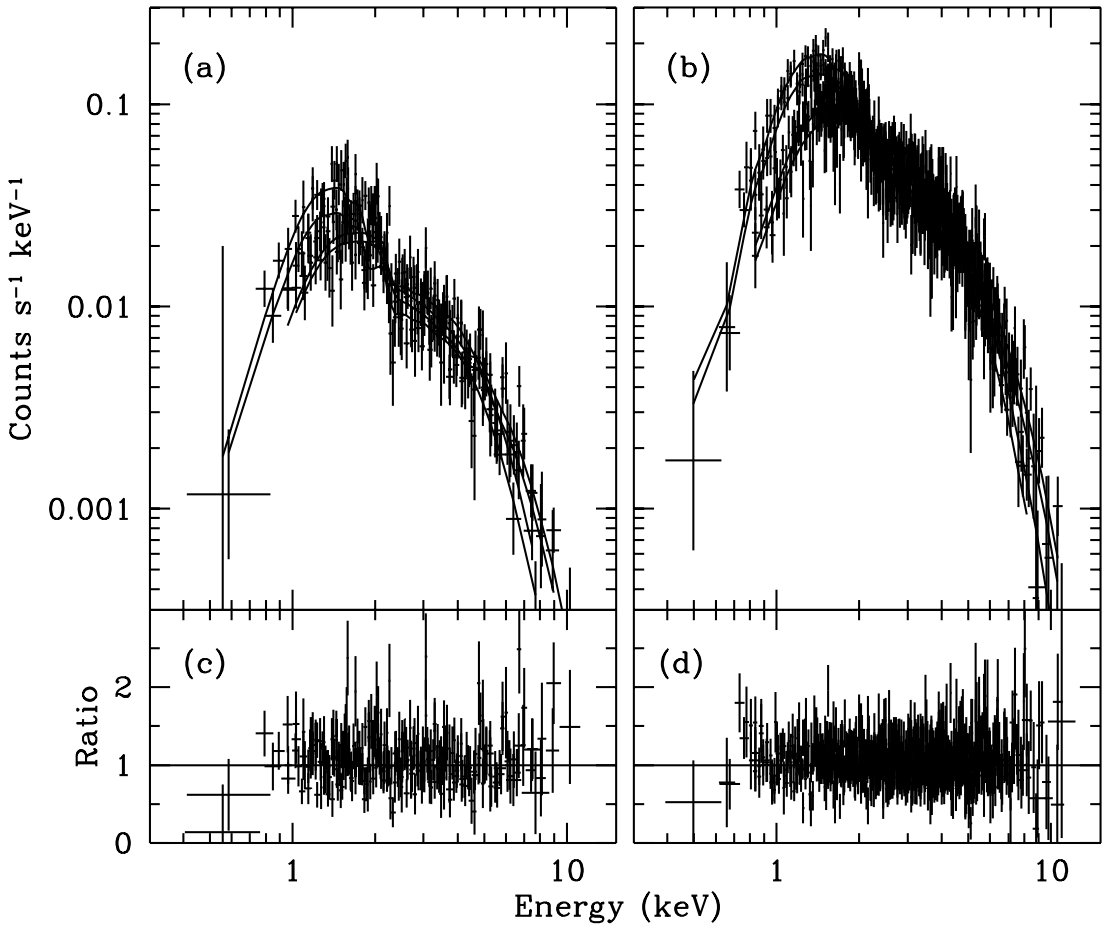

FIG. 1.—*ASCA* spectra of PKS 0528+134 in 1994 August ([*a*] and [*c*]) and 1995 March ([*b*] and [*d*]). Data from the four detectors were fitted jointly with a single power law plus free absorption. (*a*) and (*b*): Data and folded model; (*c*) and (*d*): residuals of the model, plotted as the ratio of data to model. Flux increased by a factor of ~4 between 1994 August and 1995 March, without appreciable change of spectral slope ($\Gamma \sim 1.7$–1.8).

blazars do not exhibit strong Fe features in their X-ray spectra (Ohashi et al. 1989).

2.4. *Previous X-Ray Observations*

PKS 0528+134 was observed previously in soft X-rays once with the *Einstein* IPC and twice with the *ROSAT* PSPC. The IPC observations yielded only 40 counts; nevertheless, the spectrum is consistent, within very large uncertainties, with $N_{\rm H} \sim 1.7 \times 10^{21}$ cm^{-2}, $\Gamma \sim 2.6$, and $F_{1\ \rm keV} \sim 0.1$ μJy (Bregman et al. 1985).

The source was significantly detected with *ROSAT* in 1991 March and 1992 September, with ~270 and 385 counts, respectively (Zhang et al. 1994; Mukherjee et al. 1996). In order to compare directly the *ASCA* column densities to those derived from *ROSAT*, we reanalyzed the two archival PSPC spectra. We corrected the data for the spatial gain variations using the "PCSASSCOR" script (*ROSAT* Status Report, No. 137, April 1, 1996) and rebinned the spectra over the channel range 12–211 (energy range 0.14–2.13 keV) in order to have at least 20 counts per new bin. The 1991 March data were fitted with the "pspcb–gain1–256" matrix, as appropriate for data taken in high–gain mode (before 1991 October), while the matrix "pspcb–gain2–256" was used for the observation of 1992 September.

The data were fitted with a single power law plus free absorption. For the 1991 March observation, the fit yields $N_{\rm H} = 8.54^{+6.46}_{-4.04} \times 10^{21}$ cm^{-2}, $\Gamma = 3.35^{+2.35}_{-1.85}$, and $F_{1\ \rm keV} = 1.6(<7.2)$ μJy, $\chi^2_r = 1.02/17$, with errors at 90% confidence for one parameter of interest. For the 1992 September observation, the fit with the same model yields $N_{\rm H} = 9.37^{+5.63}_{-3.97} \times 10^{21}$ cm^{-2}, $\Gamma = 3.61^{+2.19}_{-1.64}$, and $F_{1\ \rm keV} = 2.5(<9.6)$ μJy, $\chi^2_r = 1.02/17$. These values are consistent within the errors with those reported by Zhang et al. (1994) and Mukherjee et al. (1996). In neither *ROSAT* spectrum is it possible to constrain the location of the extra absorber. The unabsorbed (incident) fluxes in 0.1–2.1 keV are $\sim 5.2 \times 10^{-11}$ and 1.6×10^{-10} ergs cm^{-2} s^{-1} for the 1991 March and 1992 September data, respectively.

The *ROSAT* data, which cover softer energies than the *ASCA* SIS, are consistent with higher column densities ($N_{\rm H} \sim 10^{22}$ cm^{-2}) and steeper photon indices ($\Gamma \sim 3$) than *ASCA*, although within very large uncertainties. Since the presence of a steeper low-energy component is very important for theoretical models attempting to explain the broadband spectrum (see below), we looked carefully for the presence of any soft excess in the joint *ROSAT* and *ASCA* data. We fitted the 0.1–10 keV spectrum with a broken power law with both fixed and free $N_{\rm H}$; in both cases, no improvements of the χ^2 statistics were found. The fit is not sensitive to the choice of the low-energy photon index, with the same χ^2 obtained for Γ_1 spanning the range -3 to 10. We conclude that there is no evidence in our data for a steep component at the low energies, although it cannot be defi-

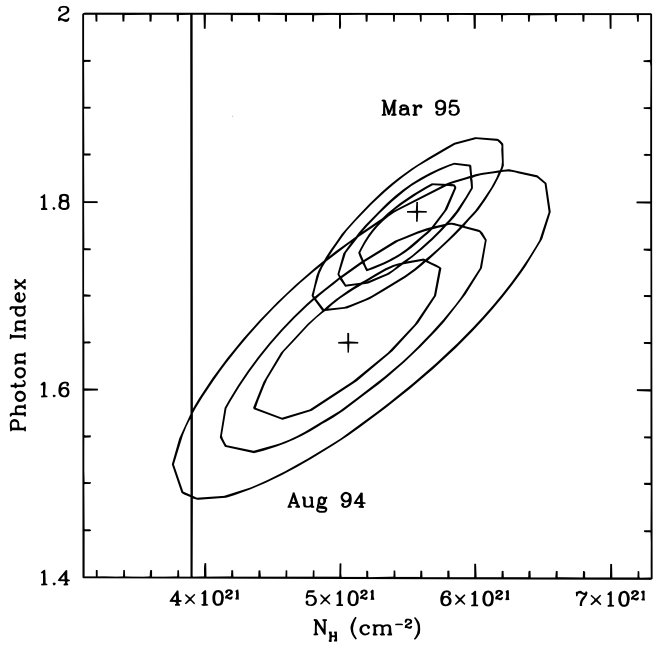

FIG. 2.—Confidence contours for the column density and the photon index from the fits to the *ASCA* spectra of PKS 0528+134 in 1994 August and 1995 March with a single power law + free N_H. Levels of 68%, 90%, and 99% for two parameters of interest ($\Delta\chi^2 = 2.3$, 4.6, 9.3) are shown. Vertical line marks the value of the total atomic + molecular Galactic N_H in the direction to the source. Fitted absorption exceeds the Galactic value at ~95% in the 1994 data set and at more than 99% in the 1995 data set. Although the flux increased by a factor of 4 from 1994 August to 1995 March, there is no large slope evolution; the maximum change of the photon index is ~0.4 at 99% confidence, or 0.2 for a fixed N_H.

nitely ruled out due to the large errors of the *ROSAT* PSPC. Observations with SAX, AXAF, and the next generation of X-ray instruments with improved sensitivity at the soft X-ray energies will allow a detailed study of the $\lesssim 1$ keV spectrum of PKS 0528+134.

The joint *ROSAT* and *ASCA* data are well described by a single absorbed power law with fitted column densities and slopes entirely consistent with the ones derived from the *ASCA* data alone in Table 2, with reduced χ^2s of 0.89/692 (both *ROSAT* spectra and *ASCA* high state) and 1.05/272 (both *ROSAT* spectra and *ASCA* low state). We conclude that a single power law with a photon index $\Gamma \sim 1.7$ and column density $\sim 5 \times 10^{21}$ cm^{-2} is an adequate representation of the *ROSAT* and *ASCA* data of PKS 0528+134.

PKS 0528+134 was detected in the *ROSAT* All-Sky Survey (RASS) with an observed flux in 0.1–2.4 keV energy range of $\sim 3.2 \times 10^{-12}$ ergs cm^{-2} s^{-1} (Brinkman et al. 1995). In order to compare the flux from the RASS with the pointed *ROSAT* PSPC observations, we used the same model as Brinkman et al., i.e., a single power law with photon index $\Gamma = 2.13$ and Galactic N_H. We obtain 0.1–2.4 keV fluxes of 0.9×10^{-12} and 1.1×10^{-12} ergs cm^{-2} s^{-1} for the 1991 March and 1992 September data, respectively. The source was a factor of 3 brighter during the RASS than at the epoch of both pointed observations.

3. OBSERVATIONS SIMULTANEOUS TO THE *ASCA* POINTING OF 1994 AUGUST

3.1. *Optical Observations*

Optical data were obtained at the 2.2 m telescope of the Calar Alto Observatory using a TEK 1024 chip with a plate scale of 0.″3 pixel^{-1}. A monitoring campaign was set up to search for variations of the optical radiation from PKS 0528+134 during the epoch of coordinated high-energy observations. Data were taken during nine consecutive nights in 1994 August (JD 2,449,573−2,449,582). During the observation, PKS 0528+134 rose shortly before dawn, limiting the accessible period to about 10 minutes per night. Two frames were taken each night in the $R(\lambda = 0.7\ \mu\text{m})$ filter. Following standard reduction, all frames were investigated for variability during the 9 day period. No variations down to the 6% level were found. Absolute calibrations were carried out during two nights of photometric quality. The large air mass (2.7–3, depending on the amount of haze near the horizon on different nights) during the observations of PKS 0528+134 introduced a large error. We derived an average brightness of $R = 20.8 \pm 0.3$ mag.

The extinction was calculated using the N_H from the fit to the 1994 August *ASCA* data (Table 2) and assuming $A_V/E(B-V) = 3.09 \pm 0.06$ (Rieke & Lebofsky 1985), $N_H/E(B-V) = 5.2 \times 10^{21}$ cm^{-2} mag^{-1} (Shull & Van Steenberg 1985), and the extinction curves of Cardelli, Clayton, & Mathis (1989). This yielded $A_V = 3.01$ and $A_R = 2.4$. The dereddened R flux is 0.13 ± 0.04 mJy.

3.2. *EGRET Observations*

PKS 0528+134 was observed with the EGRET experiment (e.g., Fichtel 1994) on board *CGRO* during viewing period VP337 (1994 August 9–29), overlapping with our *ASCA* observations of 1994 August 28. The source was detected with a significance of 3 σ. The EGRET data were analyzed using the standard EGRET data processing techniques (Bertsch et al. 1989). In order to determine the background-subtracted spectrum, the energy range 30 MeV–10 GeV was divided into 10 energy intervals, and maps of photons and exposures were made for each of the energy ranges. Likelihood analysis was used to estimate the number of source photons in each of the 10 energy bins (Mattox et al. 1996). The data were fitted to a single power-law model, $F(E) = k(E/E_0)^{-\Gamma}$, where the energy normalization factor, E_0, is chosen such that the statistical errors in the power-law index and the overall normalization are minimally correlated. In this case, $E_0 = 135$ MeV. The fitted photon index is $\Gamma = 2.68 \pm 0.44$, and the normalization constant is $(2.15 \pm 0.57) \times 10^{-9}$ photons cm^{-2} s^{-1} MeV^{-1} (errors at 1 σ, or ~68% confidence).

In 1994 August, the source was in the lowest states detected thus far. The flux integrated in 100 MeV–30 GeV is $(3.2 \pm 1.0) \times 10^{-7}$ photons cm^{-2} s^{-1}, a factor of 10 lower than during the flare of 1993 March (Mukherjee et al. 1996). The steep spectral index, $\Gamma \sim 2.7$, is in agreement with the marginal evidence that the γ-ray spectrum softens with fading intensity, as derived from the comparison of the historical low- and high-EGRET states (Mukherjee et al. 1996).

4. THE SPECTRAL ENERGY DISTRIBUTION OF PKS 0528+134

In Figure 3, we present the spectral energy distribution of PKS 0528+134 from radio to γ-rays. Apparent source luminosities, obtained assuming isotropic emission, are plotted versus rest-frame frequencies, i.e., $\nu_{\rm obs}(1+z)$. The simultaneous *ASCA*, EGRET, and optical data of 1994 August are plotted as filled points and hatched areas, with 90% and 68% confidence errors on X-ray and γ-ray data, respectively.

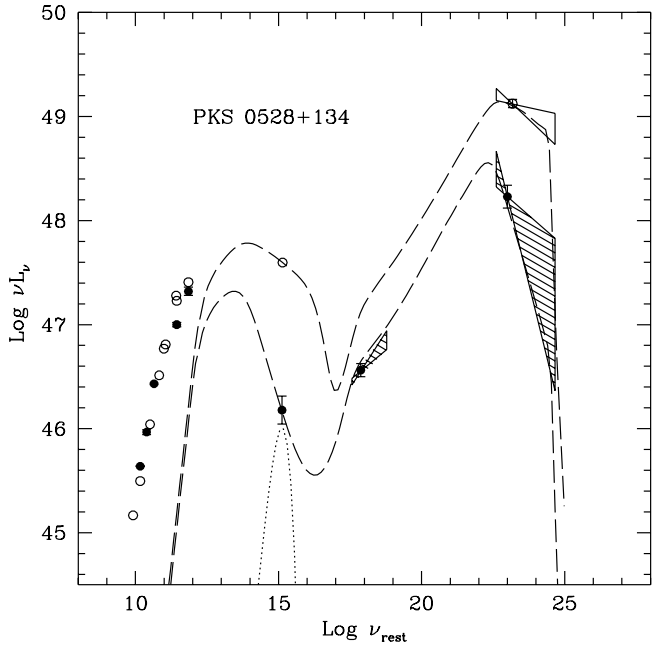

FIG. 3.—Spectral energy distribution of PKS 0528+134 from radio to γ-rays in the rest frame of the source. *Filled circles and hatched areas*: Simultaneous spectral energy distribution of 1994 August. Radio and millimeter data are within 1 month of the simultaneous *ASCA*, EGRET, and optical observations (see text). *Open symbols*: Simultaneous spectral energy distribution during the γ-ray flare of 1993 March (from Mukherjee et al. 1996). Optical fluxes have been dereddened using $A_V = 3$, derived from the *ASCA* data (see text). EGRET flux measured in 1994 August is an order of magnitude lower than in 1993 March; variability of larger amplitude is present in the optical band. *Dashed lines*: Spectral energy distributions predicted by a synchrotron plus external Compton scattering model whose input parameters are reported in Table 3. Spectrum of the external photons is also shown (*dotted line*).

We searched the literature and public databases for published flux densities at radio and millimeter frequencies taken as close as possible to our 1994 August observations. In the radio band, the source is the target of an intensive monitoring with the University of Michigan 26 m single-dish telescope; the measurements are available on-line from the University of Michigan Radio Astronomy database (Aller et al. 1985). Flux densities at 4.8, 8.0, and 14.5 GHz were obtained in 1994 September 9, August 30, and August 27, respectively (3.36 ± 0.03, 4.29 ± 0.10, and 6.90 ± 0.13 mJy, respectively). As a part of a monitoring program at millimeter frequencies, the source was also observed at 90 and 230 GHz in 1994 December 12 and 1994 October 1, respectively, with the Swedish ESO Telescope; the fluxes are published in Mukherjee et al. (1996). These contemporaneous radio and millimeter flux densities are plotted as filled circles in Figure 3.

For comparison, in Figure 3 we show the broadband spectrum obtained during the γ-ray flare of 1993 March (Mukherjee et al. 1996). The radio and optical flux densities (*open symbols*) were measured within 1 month of the EGRET flare. In the optical, the flux density has been dereddened with the same extinction used for the 1994 August, i.e., $A_R = 2.4$ (assuming the latter did not change; see below).

Two distinct spectral components are clearly present in Figure 3. The radio through optical emission has a peak somewhere in the region between the millimeter and the optical data, where, unfortunately, there are no data at present. From a parabolic interpolation to the data for the 1994 August epoch, we derive a peak frequency $\nu_p = 1.1 \times 10^{13}$ Hz and peak luminosity $\nu_p L_p = 4.4 \times 10^{47}$ ergs s^{-1}, while the luminosity integrated between 10^9 and 10^{16} Hz is $L_B = 2.4 \times 10^{48}$ ergs s^{-1}. At higher energies, the *ASCA* and EGRET data (*hatched areas*) form a separate spectral component with a sharp peak around $\sim 10^{22}$ Hz frequencies. In this case, the parabolic interpolation does not provide an adequate description of the data. A simple integration of the area below the *ASCA* and EGRET data from 10^{17} to 10^{25} Hz, using the spectral parameters derived above, yields a bolometric luminosity of the order of $\approx 10^{49}$ ergs s^{-1}. Although these numbers are only rough estimates likely affected by large errors due to the incomplete coverage of the spectral distribution, they show that in PKS 0528+134 the power emitted at the higher energies is larger than at lower frequencies, even during a low state.

PKS 0528+134 can vary by as much as a factor of 3 over timescales of months to years at cm and mm frequencies (Aller et al. 1985; Steppe et al. 1993; Zhang et al. 1994; Mukherjee et al. 1996). However, no flux changes occurred at low frequencies in Figure 3 from 1993 March to 1994 August. Instead, large variability is present at both optical and γ-ray energies. The EGRET flux decreased by a factor of 10 from 1993 March to 1994 August, while in the optical the flux density decreased by a larger factor. We discuss this result further in § 6.2.

Interestingly, spectral variability in PKS 0528+134 seems more pronounced in the γ-ray range than at X-rays. No significant spectral changes accompany the X-ray flux increase of a factor of 4 between the *ASCA* observations of 1994 August and 1995 March (§ 2.2), while at MeV energies the increase of the flux is accompanied by some flattening of the spectrum (Mukherjee et al. 1996). Following this trend, we expect that the EGRET data taken in 1995 March would correspond to a higher flux and flatter spectrum than the EGRET data in 1994 August. The analysis of these data is in progress (Collmar et al. 1996).

5. SUMMARY OF THE OBSERVATIONAL RESULTS

We have presented two *ASCA* spectra of PKS 0528+134 obtained at two separate epochs in 1994 August and 1995 March, which represent the first measurement of the X-ray continuum in a medium-hard energy range for this blazar. Optical and EGRET observations contemporaneous to the 1994 *ASCA* data set have also been discussed. Our major findings are as follows:

1. Both *ASCA* spectra are well-fitted with a single power-law model with photon index $\Gamma \sim 1.7$–1.8 and with a fitted column density of $\sim 5 \times 10^{21}$ cm^{-2}. The latter is at least $\Delta N_H \sim 1 \times 10^{21}$ cm^{-2} in excess of the Galactic value (99% confidence). There is no statistical preference for a local ($z = 0$), rest frame ($z = 2.07$), or intervening absorber.

2. The *ASCA* flux increased by a factor of 4 in ~ 7 months, from 1994 August to 1995 March, without appreciable spectral change, $\Delta\Gamma \lesssim 0.2$.

3. During the EGRET observation of 1994 August, the source was in a lower γ-ray state than in any previous observation, with a flux $F(>100$ MeV$) \sim 3.2 \times 10^{-7}$ photons cm^{-2} s^{-1}, and had the steepest spectrum ($\Gamma \sim 2.7$), confirming the earlier report that the γ-ray spectrum tends to become flatter when the flux increases.

4. The *ASCA* and EGRET data during the faint state of 1994 August form a unique spectral component that requires a sharp break ($\Delta\Gamma \sim 1.15$) at $\sim$45 MeV.

5. While no flux changes occurred in the radio and millimeter bands, large variability (more than a factor of 10) is present in the optical band comparing the low state of 1994 August to the flare state of 1993 March.

6. The bulk of the power in PKS 0528+134 is emitted at γ-rays, even during a low state.

6. DISCUSSION

6.1. *X-Ray Absorption toward PKS 0528+134*

Since PKS 0528+134 is at a low-Galactic latitude, $b = -11°$, the amount of absorption caused by neutral atomic hydrogen gas in the direction of PKS 0528+134 is large, 2.6×10^{21} cm^{-2} (from the Bell Labs 21 cm maps of H I; Stark et al. 1992), with estimated uncertainties around 10^{20} cm^{-2} (Elvis, Lockman, & Wilkes 1989). In addition, the line of sight to PKS 0528+134 intersects the outer edge of the molecular cloud Barnard 30 in the λ Orion ring of clouds. The CO emission-line intensity, 2.3 K km s^{-1} (Listz & Wilson 1993), implies a column density of molecular hydrogen $N_H 2 \sim 1.3 \times 10^{21}$ atoms cm^{-2} (Bania, Marscher, & Barvainis 1991). The total atomic plus molecular absorbing column density of hydrogen in the direction of PKS 0528+134 is therefore $\sim 3.9 \times 10^{21}$ cm^{-2} (see also Zhang et al. 1994).

The strong dependence of the diffuse Galactic dust emission at 100 μm upon the total amount of atomic and molecular cold gas (Boulanger & Perault 1988) allows an independent estimate of the Galactic column density in the direction of PKS 0528+134. From the *IRAS* map at 100 μm (available electronically) and assuming a conversion factor of $N_H = 0.86 \times 10^{20}$ MJy sr^{-1} cm^{-2}, we derive $N_H \sim 3.1 \times 10^{21}$ cm^{-2}, in good agreement with the radio measurements.

The *ASCA* data of PKS 0528+134 are consistent with an observed absorption column densities of $\sim 5 \times 10^{21}$ cm^{-2}, in excess of the total atomic plus molecular Galactic column density by at least 10^{21} cm^{-2} in the observer rest frame (§ 2). This is an effect of 20% (at 99% confidence; Fig. 2), which could probably be reconciled with the uncertainties on the CO to H2 ratio (Bania et al. 1991) and on the opacity of the neutral hydrogen gas in the direction of PKS 0528+134, especially since the source is at low-Galactic latitudes. However, it is instructive to explore viable physical scenarios that could explain a possible extra absorber in the X-rays, especially because the column density scales such as $(1 + z)^{8/3}$ and the excess N_H could therefore be conspicuous at high redshifts. Below we discuss possible locations of the extra absorber locally in the Galaxy ($z = 0$), in the rest frame of the source ($z = 2.07$), or in between.

An absorption system of low-ionization lines (Al II, Al III, Fe II, and possibly Si II) is actually present at $z = 1.57$ along the line of sight to PKS 0528+134 (Hunter et al. 1993). At such a redshift, the absorber would have an equivalent column density N_H about a few $\times 10^{22}$ cm^{-2}, which would put the absorber in the regime of heavy element and damped Lyα systems (e.g., Steidel 1992). Indeed, it would be one of the nearest and gas richest systems known thus far (Lanzetta et al. 1991).

We can derive constraints on the metallicity of the intervening system from the X-ray data. To this purpose, we fitted the 1995 March *ASCA* data, which have a higher signal-to-noise ratio, with a power law with two absorption systems: one at $z = 0$ fixed at 3.9×10^{21} cm, to allow for the Galaxy absorption; the second absorber at $z = 1.57$, with the abundances of the various elements as parameters of interest in the fit. Since oxygen and carbon are redshifted out of the *ASCA* range, we can only infer the abundance of iron, the next most abundant element responsible for X-ray absorption (e.g., Morrison & McCammon 1983). From the data, we derive an abundance of iron relative to hydrogen of $N/N_H = (1.3 \pm 0.7) \times 10^{-4}$, which, for $N_H \sim 10^{22}$ cm^{-2}, implies $N_{Fe} = (1.3 \pm 0.7) \times 10^{18}$ cm^{-2} (90% confidence errors). The *ROSAT* data are, in principle, useful to derive constraints on the abundance of oxygen, while, for $z = 1.57$, carbon is redshifted out of the PSPC sensitivity range. Because of the poor resolution of the PSPC, we can only derive a 90% confidence upper limit of the oxygen column density, $N_O < 2 \times 10^{19}$ cm^{-2} (corresponding to $N_O/N_H = 2 \times 10^{-3}$).

Alternatively, the extra absorber could be located in or near the molecular cloud Barnard 30 that lies between us and PKS 0528+134. We note that radio spectra of Barnard 30 indicate unusually large abundances of HCO^+ and HCN with respect to CO (Hogerheijde et al. 1995). This is intriguing since carbon and oxygen are the elements principally responsible for the X-ray absorption below 1 keV. The excess absorption could be due to passage of clumpy material across the line of sight, as seems to be the case for the radio-loud quasar NRAO 140 (Turner et al. 1995; Marscher 1988). Turbulent motion can indeed be present inside Barnard 30 (Hogerheijde et al. 1995). Dense plasma clouds could also be passing occasionally in front of Barnard 30, as suggested by radio observations of PKS 0528+134, in which the observed low-frequency flux fluctuations have been interpreted being the result of extreme scattering events (Pohl et al. 1996).

In the latter scenario, we would expect to observe variable absorption in the direction of PKS 0528+134 in both radio and X-ray spectra at different epochs, as is the case in X-rays for NRAO 140. The two *ASCA* spectra of PKS 0528+134, taken 7 months apart, yield similar column densities, although the observation of 1994 August, corresponding to a fainter state, is affected by large uncertainties. Previous *ROSAT* observations indicate much higher column densities than *ASCA*, but, again, the measured uncertainties are large. An earlier *Einstein* IPC spectrum was consistent with $N_H \sim 1.7 \times 10^{21}$ cm^{-2} (Bregman et al. 1985), based, however, on a detection of only 40 counts. Therefore, there is no convincing evidence of variability of the X-ray absorption column densities in PKS 0528+134 based on the presently available data. Future repeated X-ray observations with high sensitivity at soft X-ray energies (e.g., SAX, AXAF, XMM), together with (possibly coordinated) radio spectrometry, would help clarifying this point.

A third possibility is an intrinsic absorber. The X-ray emission of PKS 0528+134 could be blocked by a large (N_H is about a few $\times 10^{22}$ cm^{-2}) amount of cold gas in the blazar's rest frame. Such highly opaque material would leave distinct spectral features imprinted on the X-ray spectrum (Fe emission lines, Compton "hump") at rest-frame energies $\gtrsim 6$ keV. We do not detect any feature in the *ASCA* spectra of PKS 0528+134 in the range of sensitivity of the SIS (§ 2). However, the absence of Fe lines is expected if the

source is beamed (Yaqoob et al. 1993), as is almost certainly the case in PKS 0528+134 (§ 1; see also below).

PKS 0528+134 would not be the first high-redshift quasar in which excess absorption has been observed in X-rays. Spectral flattening, attributed to intrinsic absorption in the quasar's rest frame, has been observed in the *ROSAT* PSPC data of two radio-loud quasars, PKS 0438−436 and PKS 2126−158 at $z = 2.85$ and 3.27, respectively (Elvis et al. 1994). *ASCA* observations of the latter two objects are equally consistent with an absorbed power law or with a convex broken power law with Galactic $N_{\rm H}$ and a very flat low-energy spectral index (Serlemitsos et al. 1994). Serlemitsos et al. (1994) argue that an intrinsically convex continuum (caused by synchrotron losses) may be an alternative scenario to absorption. We note, however, that synchrotron spectra are usually associated with steeper continua ($\Gamma > 2$) than measured for these objects and for PKS 0528+134. In addition, the analysis of the broadband spectral energy distribution shows that, at least in the case of PKS 0528+134, a synchrotron origin of the X-rays seems to be excluded (§ 6.2.2; see also § 2.4).

In summary, the *ASCA* data measure excess absorption with respect to the total Galactic $N_{\rm H}$ toward PKS 0528+134, with $\Delta N_{\rm H}(z = 0) \sim 1 \times 10^{21}$ cm^{-2}. The absorption may take place in the source's rest frame, in which case the presence of associated features like the Fe emission lines could be swamped by the beamed continuum, or intervening (Lyα damped systems), or locally in the Galactic molecular cloud obscuring the line of sight to the blazar. The latter would be related to clumpy material inside or nearby the molecular cloud, and variable X-ray as well as radio column densities would be expected.

6.2. *The High-Energy Continuum Emission of PKS 0528+134*

There is now strong evidence that the smooth, highly variable, and polarized radio through optical/UV continuum of blazars is synchrotron emission from plasma in relativistic motion. The emission at higher energies is attributed to inverse Compton scattering of the same synchrotron photons (synchrotron self-Compton, SSC; Maraschi, Ghisellini, & Celotti 1992) or/and of seed photons external to the synchrotron-emitting region (external Compton, EC; Dermer, Schlickeiser, & Mastichiadis 1992; Sikora, Begelman, & Rees 1994; Ghisellini & Madau 1996).

Irrespective of the source of the seed photons, however, in the observed spectra there must be a close correspondence between the synchrotron and Compton fluxes due to the fact that the same relativistic electrons lose energy through both mechanisms. In the context of the homogeneous model, if ν_S is the peak of the synchrotron component, there must be a second peak in the spectrum corresponding to the upscattered synchrotron photons at $\nu_{\rm C} \propto \gamma_b^2 \nu_S$ in the SSC model and $\propto \gamma_b^2 \Gamma \nu_{\rm ext}$ in the EC model, where γ_b is the break energy of the electrons, and Γ and $\nu_{\rm ext}$ are the electron Lorentz factor and the frequency of the external photons, respectively. The variability of the synchrotron and Compton fluxes must be strongly correlated. Specifically, since the variability of the synchrotron spectrum is more pronounced above the peak, we expect large variability above the peak of the Compton emission.

Applying these arguments to the spectral energy distribution of PKS 0528+134 in Figure 3, we identify $\nu_S \sim 10^{13}$ Hz and $\nu_{\rm C} \sim 10^{22}$ Hz for the low state of 1994 August (§ 4). The fact that the synchrotron and inverse Compton spectra must be homologous therefore implies that the GeV photons are produced by the same electrons that emit synchrotron IR/optical photons, while the X-ray emission is linked to the submillimeter/millimeter part of the synchrotron component. Since the EGRET data are above the peak of the emission, larger flux and spectral variability at MeV energies than in the X-rays are expected, as is indeed observed. The large variability amplitude in the optical is also expected, as these data lie well above the synchrotron peak, where the variability is more pronounced.

The synchrotron and inverse Compton mechanisms are therefore the most likely processes to account for the radio-to-γ-ray emission of PKS 0528+134. Application of specific SSC and EC models to the spectral distribution in Figure 3 are examined in turn in the following sections.

6.2.1. *Synchrotron Self-Compton Models for PKS 0528+134*

In a pure SSC (one zone) scenario, with the above values of the synchrotron and Compton peaks, one derives that the electrons responsible for most of the emission at the peaks have Lorentz factors $\gamma_b \sim (\nu_{\rm C}/\nu_S)^{1/2} \sim 3 \times 10^4 (\nu_{C,22}/\nu_{S,13})^{1/2}$, where $\nu_S = 10^{13} \nu_{S,13}$ Hz and $\nu_{C,22} = 10^{22} \nu_{\rm C}$ Hz. This in turn implies a very small value of the magnetic field,

$$B = \frac{1+z}{\delta} \frac{\nu_S^2}{3.7 \times 10^6 \nu_{\rm C}} \sim \frac{8 \times 10^{-3}}{\delta} \frac{\nu_{S,13}^2}{\nu_{C,22}} \ {\rm G} \ . \qquad (1)$$

In a pure SSC scenario, the magnetic-to-intrinsic radiation energy density (the latter denoted by U'_S) must be approximately equal to the ratio of the synchrotron to Compton luminosity, $L_S/L_{\rm C}$, which is about 1/20 for PKS 0528+134 (Fig. 3). The presence of small magnetic fields then implies a small radiation energy density of the synchrotron radiation, allowed only for very large dimensions of the emitting region (with problems with the short variability timescale) or for huge values of the beaming factors (see Ghisellini & Maraschi 1996). Using

$$\frac{L_S}{L_{\rm C}} = \frac{U_B}{U'_S} \sim \frac{4\pi R_{\rm blob}^2 c U_B \delta^4}{L_S} \ , \qquad (2)$$

one derives, for $L_S/L_{\rm C} \sim 1/20$,

$$R_{\rm blob} \delta \sim 7 \times 10^{19} L_{S,47}^{1/2} \frac{\nu_{C,22}}{\nu_{S,13}^2} \ {\rm cm} \ , \qquad (3)$$

where $L_S = 10^{47} L_{S,47}$ ergs s^{-1}. These estimates argue against a pure SSC origin of the high-energy spectrum of PKS 0528+134.

On the other hand, given the scaling with ν_S of the above relations, one finds that the SSC model is viable if $\nu_S > 10^{14}$ Hz.

Assuming that the amount of the extinction is $A_V \sim 5$ (from the best-fit $N_{\rm H}$ derived from the *ROSAT* data, see above) and that the peak of the synchrotron emission is in the optical band, we can interpret the overall spectra of the source with a SSC model. In this scenario, the change in the overall luminosity is accompanied by a change of the magnetic field in order to maintain a constant ratio of the radiation to magnetic energy density. Assuming $R = 3 \times 10^{16}$ cm and $\delta = 17$, we find that the break in the electron distribution is at $\gamma_b = 5000$, while the magnetic field value is

between 0.6 and 1.9 G. The relatively high value of δ is fixed by the above relations and by the observed short variability timescale. Since, in this case, the synchrotron spectrum extends up to soft X-rays, the SSC model could explain a steepening of the X-ray spectrum to small energies (below ~ 1 keV).

6.2.2. *External Compton Scattering in PKS 0528+134*

The only optical spectrum published so far for PKS 0528+134 (Hunter et al. 1993) exhibits a prominent redshifted emission line of C IV (equivalent width 41 Å). We reanalyzed this spectrum in order to derive the line flux, which directly gives the external radiation luminosity, $L_{\rm BLR}$. This analysis is described in the Appendix.

The ratio of the external photon density, $U'_{\rm BLR}$, to the synchrotron photon density, U'_S, is (in the rest frame of a synchrotron-emitting blob)

$$\frac{U'_{\rm BLR}}{U'_S} \sim \delta^4 \Gamma^2 \frac{L_{\rm BLR}}{L_S} \frac{R^2_{\rm blob}}{R^2_{\rm BLR}}, \quad (4)$$

where $R_{\rm blob}$ and $R_{\rm BLR}$ are the radii of the blob and of the region emitting the optical lines, respectively, δ is the Doppler factor, and Γ is the bulk Lorentz factor of the emitting plasma. We derive $L_{\rm BLR} = (0.5\text{–}20) \times 10^{46}$ ergs s^{-1} (allowing for the calibration uncertainty of the optical spectrum; see Appendix) and $L_S \sim 4.4 \times 10^{47}$ ergs s^{-1} from § 4 (luminosity at the synchrotron peak frequency in 1994 August). Note that the lower limit on the beaming factor in order to avoid γ-γ absorption is $\delta > 5.8$ (Dondi & Ghisellini 1994).

Assuming the lowest value for $L_{\rm LBR}$, $\delta = 5.8$, $\Gamma \sim 10$, and $R_{\rm blob} \sim 10^{16}$ cm (as suggested by the about a few days variability timescale in γ-rays; § 1), the radiation density is dominated by the broad-line photons as long as $R_{\rm BLR} \lesssim 5 \times 10^{17}$ cm. This value of the broad-line region size is relaxed if δ is allowed to be higher. Moreover, the fitted slope of the optical spectrum is fairly flat, $\alpha_\nu \sim 0.2$ (see Appendix), possibly indicating the presence of excess blue emission in the rest frame. These arguments show that in PKS 0528+134 there may be a nonnegligible contribution of an external radiation field.

As discussed above, in PKS 0528+134 the γ-ray flux exceeds the optical flux, even in the low state, which also indicates that the EC scattering may be the dominant cooling mechanism. An important caveat, however, is that the γ-ray-to-optical flux ratio in Figure 3 is highly sensitive to the assumed extinction; for A_V larger than 3 (the value used here, see above), the synchrotron peak moves in the optical region and the SSC mechanism is viable. Here we used the extinction derived from our *ASCA* measurements, since these represent the most precise determination of the $N_{\rm H}$ and therefore of A_V obtained so far. Indeed, dereddening their optical magnitude with $A_V = 5$, Mukherjee et al. (1996) find that the SSC model reproduces well the spectral energy distribution of 1993 March. However, this value was derived from the *ROSAT* data, which are affected by large uncertainties (§ 2).

To model the spectral energy distributions in Figure 3, we assumed that the radio through UV emission is synchrotron radiation from a relativistic electron population in a homogeneous region, and that the high-energy continuum is produced by upscattering of external seed photons off the same electrons. These external photons have a narrow energy distribution around a typical frequency $\approx 10^{15}$ Hz (*dotted line curve*, Fig. 3). The emission region is filled with a uniform plasma of electrons of random energy γ and constant bulk motion with Lorentz factor Γ in a constant magnetic field B. We assumed a region of size $R = 3 \times 10^{16}$ cm and a continuous injection of relativistic electrons between $\gamma_{\rm min} = 300$ and $\gamma_{\rm max} = 7000$, distributed in energy as a single power law ($\propto \gamma^{-s}$). The steady particle distribution is computed self-consistently considering radiative cooling (including the effects of the Klein–Nishina cross section), escape, and pair production. However, the latter two effects are negligible, since cooling is faster than escape at all energies, and the steepness of the primary γ-ray spectrum makes the reprocessing due to pairs unimportant. On the other hand, the sharp cut-off at the end of the γ-ray spectrum is a result of the absorption of γ-rays colliding with the external photons.

Table 3 lists the parameters assumed to reproduce the low state of 1994 August and the high state of 1993 March. These solutions are plotted on the data in Figure 3 (*dashed lines*). The solution does not reproduce the radio and millimeter data, which are expected to come from more extended regions.

Given the limited data available, we are able to explain complex spectral changes across more than 10 decades in frequency with a few reasonable changes of model parameters. The lower state of 1994 August is obtained for an injected spectrum $s = -3.9$ and injected compactness $\ell = 1.5$, corresponding to a luminosity of 5.5×10^{44} ergs s^{-1}. To reproduce the higher state of 1993 March, we increased both the injected luminosity (by a factor of 3) and the beaming factor; in addition, the injected electron spectrum flattens.

A prediction of the EC model is that the blue-bump contribution in the optical should become more and more important in low-intensity states (Fig. 3). Our estimate of the spectral slope of the Hunter et al. (1993) optical spectrum yields a value $\alpha_\nu \sim 0.2$ (see Appendix), which seems to indicate the presence of excess emission at UV rest-frame frequencies. However, these optical observations correspond to a very high state of the source, although the flux estimate can be highly uncertain (see Appendix). Repeated spectroscopy of PKS 0528+134 is clearly needed to assess the existence and determine the strength of possible thermal contributions to the optical emission of PKS 0528+134.

In conclusion, we showed that inverse Compton scattering of ambient photons can play an important role in the generation of the high-energy continuum of PKS 0528+134. On the basis of the present data, however, synchrotron self-Compton scenarios cannot be definitely ruled out. As discussed above, a crucial parameter to discriminate

TABLE 3

HOMOGENEOUS EXTERNAL COMPTON MODEL

Parameter	Low State	High State	Notes
R	3×10^{16}	3×10^{16}	Region size (cm)
ℓ	0.5	1.5	Injected compactness
$\gamma_{\rm min}$	300	300	Minimum electron energy
$\gamma_{\rm max}$	7000	7000	Maximum electron energy
s	3.9	2.3	Injected electron spectrum ($\propto \gamma^{-s}$)
δ	13	15	Beaming factor
B	8	8	Magnetic field (G)

the SSC and EC models is the amount of extinction in the optical.

7. CONCLUSIONS

It is clear that PKS 0528+134 is an important target for multifrequency observations. Its γ-ray brightness together with the extreme flux and spectral variability makes this source an excellent candidate to study the mechanisms of the γ-ray production in blazars.

We have shown that Compton scattering of external photons may be the dominant electron cooling mechanism in PKS 0528+134. A critical parameter in our arguments is the amount of extinction along the line of sight to the source, which, on the basis of all the current X-ray observations, exceeds the Galactic value. This quantity rules the ratio of the γ-ray-to-optical flux and therefore the relative importance of the SSC and EC mechanisms. We have adopted the absorption derived from our *ASCA* measurements, since it is more precise than from previous *ROSAT* data; however, the *ASCA* data are not sensitive to energies below 0.5 keV. Further refinements of the absorption with current and future missions (SAX, AXAF, XMM) are highly desirable. Another critical parameter of the model is the peak frequency of the synchrotron emission. Observations in the region between the millimeter and the optical range—currently feasible with ISO—where at present there is a gap, will be particularly valuable to determine with accuracy the position of the synchrotron peak.

The location of the possible additional absorber is still an open question. Among the various possible scenarios, an intriguing possibility is that the absorber is intervening. This is corroborated by the optical evidence of a low-ionization absorption system at $z = 1.57$. If responsible for the extra X-ray absorption, then this would be one of the most massive ($N_{\rm H} \sim 10^{22}$ cm^{-2}) and closest damped Lyα systems known. *Hubble Space Telescope* spectroscopy would certainly be of great value to better study its properties; however, this observation is made difficult by the high reddening in our Galaxy in the direction to PKS 0528+134.

We are grateful to Palle Moller and Stan Hunter for allowing us to use their optical observation of PKS 0528+134, and to Margo and Hugh Aller for the University of Michigan radio data. The University of Michigan Radio Astronomy Observatory is supported by the National Science Foundation and by funds from the University of Michigan. We also acknowledge interesting conversations with Brian Espey, Greg Madejski, Palle Moller, and Richard Mushotzky, as well as with Elena Pian and Riccardo Scarpa about the analysis of the optical data. R. M. S. and C. M. U. were financially supported by an NRC Research Associate Fellowship and NASA grant NAG 5-2538, respectively. S. W. thanks J. Heidt and A. Heines for help during the observations at Calar Alto, and the DFG (DFG 328) for financial support. A. E. W. gratefully acknowledges support from the NASA Long-Term Space Astrophysics Program. This research has made use of the NASA/IPAC Extragalactic Database (NED) which is operated by the Jet Propulsion Laboratory, California Institute of Technology, under contract with the National Aeronautics and Space Administration.

APPENDIX

OPTICAL CONTINUUM SLOPE AND EMISSION LINE FLUX OF PKS 0528+134

The estimate of the external radiation field is important for a discussion of the mechanisms of the high-energy continuum production in blazars. While for several quasar-like blazars extensive optical spectrometry has been performed, for PKS 0528+134 this is made difficult by the large amount of reddening in the line of sight. Only one optical spectrum thus far was taken for this source (Hunter et al. 1993), which exhibits a prominent C IV line redshifted to λ4750 Å. We reanalyzed this spectrum with the purpose to estimate the line flux and the continuum slope.

The optical spectrum of PKS 0528+134 was calibrated only to relative units, and no correction factors were applied. Thus, the continuum level is not well known and can be uncertain to more than 2 mag (P. Moller 1996, private communication). Using the IRAF tool *splot*, we normalized the continuum and determined an equivalent width of the C IV line of 41 Å, in agreement with Hunter et al. (1993). The dereddened V magnitude (using $A_V = 3$) is 13. We fitted the dereddened spectrum in a line-free region assuming a power-law model, and we derived a slope of $\alpha = 0.18 \pm 0.08$ (where $F_\nu \propto \nu^\alpha$). The continuum measured at redshifted C IV (4750 Å) is 2.7×10^{-14} ergs cm^{-2} s^{-1} Å^{-1}, which yields a line flux of 1.1×10^{-12} ergs cm^{-2} s^{-1}. However, the estimate of the continuum and therefore of the line flux is uncertain by at least a factor of 6.

REFERENCES

Aller, H. D., et al. 1985, ApJS, 59, 513
Bania, T. M., Marscher, A. P., & Barvainis, R. 1991, AJ, 101, 2147
Bertsch, D. L., et al. 1989, in Proc. Gamma Ray Observatory Science Workshop, ed. W. N. Johnson, 2
Boulanger, F., & Perault, M. 1988, ApJ, 330, 964
Bregman, J. N., et al. 1985, ApJ, 291, 505
Brinkman, W., et al. 1995, A&AS, 109, 147
Cardelli, J. A., Clayton, G. C., & Mathis, J. S. 1989, ApJ, 345, 245
Collmar, W., Diehl, R., Lichti, G. G., Schönfelder, V., Steinle, H., & Strong, A. W. 1993, in AIP Conf. 304, Proc. Second Compton Symp., ed. C. E. Fichtel, N. Gehrels, & J. P. Norris, 659
Collmar, W., et al. 1996, in preparation
Dermer, C. D., Schlickeiser, R., & Mastichiadis, A. 1992, A&A, 256, L27
Dondi, L., & Ghisellini, G. 1995, MNRAS, 273, 583
Elvis, M., Fiore, F., Wilkes, B. J., McDowell, J., & Bechtold, J. 1994, ApJ, 422, 60
Elvis, M., Lockman, F. J., & Wilkes, B. J. 1989, AJ, 97, 777
Fichtel, C. 1994, ApJS, 90, 917
Fugmann, W., & Meisenheimer, K. 1988, A&AS, 76, 145
Ghisellini, G., & Madau, P. 1996, MNRAS, 280, 67
Ghisellini, G., & Maraschi, L. 1996, A&A, in press
Hogerheijde, M. R., de Geus, E. J., Spaans, M., van Langevelde, H. J., & van Dishoeck, E. F. 1995, ApJ, 441, L93
Hunter, S. D., et al. 1993, ApJ, 409, 134
Kerrick, A. D., et al. 1995, ApJ, 452, 588
Lanzetta, K. M., Wolfe, A. M., Turnshek, D. A., Lu, L., McMahon, R. G., & Hazard, C. 1991, ApJS, 77, 1
Liszt, H. S., & Wilson, R. W. 1993, ApJ, 403, 663
Maraschi, L., Ghisellini, G., & Celotti, A. 1992, ApJ, 397, L5
Marscher, A. P. 1988, in IAU Symp. 129, The impact of VLBI on Astrophysics and Geophysics, ed. M. J. Reid & J. M. Moran (Dordrecht: Reidel), 35

Marscher, A. P., Bloom, S. D., Zhang, Y. F., & Gear, W. K. 1994, in IAU Symp. 159, Multiwavelength Continuum Emission of AGN, ed. T. J.-L. Courvoisier & A. Blecha (Dordrecht: Reidel), 155
Mattox, J. R., et al. 1996, ApJ, 461, 396
McNaron-Brown, K., et al. 1995, ApJ, 451, 575
Morrison, R., & McCammon, D. 1983, ApJ, 270, 119
Mukherjee, R., et al. 1996, ApJ, 470, 831
Ohashi, T., et al. 1989, in Proc. 23d ESLAB Symp., Bologna, Italy (ESA SP-296
Perley, R. A. 1982, AJ, 87, 859
Pohl, M., et al. 1996, A&A, in press
Rieke, G. H., & Lebofsky, M. 1985, ApJ, 288, 618
Sambruna, R. M., Barr, P., Maraschi, L., Tagliaferri, G., & Treves, A. 1994, ApJ, 434, 468
Serlemitsos, P., Yaqoob, T., Ricker, G., Woo, J., Kunieda, H., Terashima, Y., & Iwasawa, K. 1994, PASJ, 46, L43
Shull, J. M., & Van Steenberg, M. E. 1985, ApJ, 294, 599
Sikora, M., Begelman, M. C., & Rees, M. J. 1994, ApJ, 421, 153
Stark, A. A., Gammie, C. F., Wilson, R. W., Bally, J., Linke, R. A., Heiles, C., & Hurwitz, M. 1992, ApJS, 79, 77
Steidel, C. C. 1992, PASP, 104, 843
Steppe, H., et al. 1993, A&AS, 102, 611
Tanaka, Y., Inoue, H., & Holt, S. S. 1994, PASJ, 46, L37
The ABC Guide to *ASCA* Data Reduction, v.4, 1995 March
Thompson, D. J., et al. 1995, ApJS, 101, 259
Turner, T. J., George, I. M., Madejski, G. M., Kitamoto, S., & Suzuki, T. 1995, ApJ, 445, 660
von Montigny, C., et al. 1995, ApJ, 440, 525
Wall, J. V., & Peacock, J. A. 1985, MNRAS, 216, 173
Yaqoob, T., McKernan, B., Done, C., Serlemitsos, P. J., & Weaver, K. A. 1993, ApJ, 416, L5
Zhang, Y. F., et al. 1994, ApJ, 432, 91